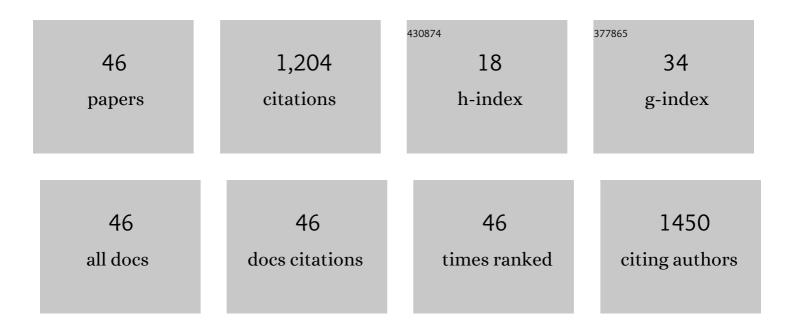
Zhiwu Chen

List of Publications by Year in descending order

Source: https://exaly.com/author-pdf/7572745/publications.pdf Version: 2024-02-01



#	Article	IF	CITATIONS
1	Tungstenâ€doped foam gâ€C ₃ N ₄ with improved photocatalytic properties for degradation of pollutant and hydrogen evolution. Journal of the American Ceramic Society, 2022, 105, 1052-1061.	3.8	7
2	In situ fabrication of niobium pentoxide/graphitic carbon nitride type-II heterojunctions for enhanced photocatalytic hydrogen evolution reaction. Journal of Colloid and Interface Science, 2022, 608, 1951-1959.	9.4	38
3	Hot-pressed (1-x)[0.9(0.3CoFe2O4-0.7BiFeO3)-0.1Pb(Zr0.52,Ti0.48)O3]-x poly(vinylidene difluoride) multiferroic composites with magnetically driven polarization. Journal of Materials Science: Materials in Electronics, 2022, 33, 4806-4818.	2.2	2
4	Piezoelectric Effect Enhanced Photocatalytic Activity of Pt/Bi3.4Gd0.6Ti3O12 Plasmonic Photocatalysis. Nanomaterials, 2022, 12, 1170.	4.1	5
5	Self-assembled synthesis of oxygen-doped g-C3N4 nanotubes in enhancement of visible-light photocatalytic hydrogen. Journal of Energy Chemistry, 2021, 54, 36-44.	12.9	111
6	Hydrothermal synthesis of tetragonal barium titanate nanopowders under moderate conditions. Processing and Application of Ceramics, 2021, 15, 179-183.	0.8	4
7	Nano-porous Al/Au skeleton to support MnO2 with enhanced performance and electrodeposition adhesion for flexible supercapacitors. RSC Advances, 2021, 11, 21405-21413.	3.6	3
8	Relationship between chemical composition, phase structure and piezoelectric property of BiFeO3–BaTiO3 ceramics near morphotropic phase boundary. Journal of Materials Science: Materials in Electronics, 2021, 32, 7719-7728.	2.2	12
9	Electrostatic coupling-driven dielectric enhancement of PZT/BTO multilayer thin films. Journal of Materials Science: Materials in Electronics, 2021, 32, 18087-18094.	2.2	0
10	Excellent piezoelectric performance of Bi-compensated 0.69BiFeO3-0.31BaTiO3 lead-free piezoceramics. Journal of Materials Science: Materials in Electronics, 2021, 32, 22637-22644.	2.2	12
11	Highly Catalytic Selectivity for Hydrogen Peroxide Generation from Oxygen Reduction on Nd-Doped BI ₄ Ti ₃ O ₁₂ Nanosheets. Journal of Physical Chemistry C, 2021, 125, 24814-24822.	3.1	16
12	Phase transition and electrical properties of BiFe0.97Ga0.03O3–BaTiO3 lead-free ceramics. Ferroelectrics, 2021, 583, 143-150.	0.6	1
13	A novel ternary MoS ₂ /MoO ₃ /TiO ₂ composite for fast photocatalytic degradation of rhodamine B under visible-light irradiation. New Journal of Chemistry, 2020, 44, 537-542.	2.8	20
14	Plasmonic Bi metal as a co-catalyst deposited on C-doped Bi6O6(OH)3(NO3)3·1.5H2O for efficient visible light photocatalysis. Journal of Photochemistry and Photobiology A: Chemistry, 2020, 389, 112290.	3.9	9
15	Multiferroic characterization of 3-phase (1-x) (0.7BiFeO3-0.3CoFe2O4)-xPb(Zr,Ti)O3 composites with magnetically driven polarization. Journal of Alloys and Compounds, 2020, 849, 156681.	5.5	10
16	Creation of oxygen vacancies to activate lanthanum-doped bismuth titanate nanosheets for efficient synchronous photocatalytic removal of Cr(VI) and methyl orange. Journal of Molecular Liquids, 2020, 314, 113613.	4.9	24
17	Improvement of surge current performances of ZnO varistor ceramics via C3N4-doping. Journal of the European Ceramic Society, 2020, 40, 2390-2395.	5.7	29
18	Synergism of oxygen vacancies, Ti3+ and N dopants on the visible-light photocatalytic activity of N-doped TiO2. Journal of Photochemistry and Photobiology A: Chemistry, 2019, 382, 111928.	3.9	25

ZHIWU CHEN

#	Article	IF	CITATIONS
19	A solid-state chemical reduction approach to synthesize graphitic carbon nitride with tunable nitrogen defects for efficient visible-light photocatalytic hydrogen evolution. Journal of Colloid and Interface Science, 2019, 535, 331-340.	9.4	79
20	Enhanced Photocatalytic Activity of Vacuumâ€activated TiO ₂ Induced by Oxygen Vacancies. Photochemistry and Photobiology, 2018, 94, 472-483.	2.5	19
21	Facile synthesis of BiFeO3 nanosheets with enhanced visible-light photocatalytic activity. Journal of Materials Science: Materials in Electronics, 2018, 29, 4817-4829.	2.2	8
22	Enhanced photocatalytic performance of Bi4Ti3O12 nanosheets synthesized by a self-catalyzed fast reaction process. Ceramics International, 2018, 44, 23014-23023.	4.8	13
23	A Facile Method for the Preparation of Colored Bi4Ti3O12â^'x Nanosheets with Enhanced Visible-Light Photocatalytic Hydrogen Evolution Activity. Nanomaterials, 2018, 8, 261.	4.1	23
24	Improved dielectric properties in A′â€site nickelâ€doped CaCu ₃ Ti ₄ O ₁₂ ceramics. Journal of the American Ceramic Society, 2017, 100, 4021-4032.	3.8	45
25	Chromium-modified Bi 4 Ti 3 O 12 photocatalyst: Application for hydrogen evolution and pollutant degradation. Applied Catalysis B: Environmental, 2016, 199, 241-251.	20.2	103
26	Enhanced photocatalytic performance over Bi4Ti3O12 nanosheets with controllable size and exposed {0 0 1} facets for Rhodamine B degradation. Applied Catalysis B: Environmental, 2016, 180, 698-706.	20.2	212
27	Ferromagnetic and photocatalytic properties of pure BiFeO3 powders synthesized by ethylene glycol assisted hydrothermal method. Journal of Materials Science: Materials in Electronics, 2015, 26, 1077-1086.	2.2	13
28	Ferromagnetism and enhanced photocatalytic activity in Nd doped BiFeO3 nanopowders. Journal of Materials Science: Materials in Electronics, 2015, 26, 9929-9940.	2.2	36
29	Solvothermal synthesis and conductive properties of nanorod-constructed Al-doped ZnO microflowers. Journal of Materials Science: Materials in Electronics, 2014, 25, 1724-1730.	2.2	11
30	Sol–gel-hydrothermal synthesis and conductive properties of Al-doped ZnO nanopowders with controllable morphology. Journal of Alloys and Compounds, 2014, 587, 692-697.	5.5	25
31	Low-temperature acetone-assisted hydrothermal synthesis and characterization of BiFeO3 powders. Journal of Materials Science: Materials in Electronics, 2014, 25, 4039-4045.	2.2	18
32	Structural, electrical and piezoelectric properties of V-, Nb- and W-substituted CaBi4Ti4O15 ceramics. Journal of Materials Science: Materials in Electronics, 2014, 25, 3396-3402.	2.2	17
33	Ethanolâ€Assisted Hydrothermal Synthesis and Characterization of <scp><scp>BiFeO</scp></scp> ₃ Nanopowders. Journal of the American Ceramic Society, 2013, 96, 1345-1348.	3.8	15
34	Lowâ€Temperature Synthesis of <scp><scp>Bi</scp></scp> _{3.15} <scp><scp>Nd</scp></scp> _{0.85} <scp><scp>Ti</scp><!--<br-->Nanoplates by a Sol–Gelâ€Hydrothermal Method. Journal of the American Ceramic Society, 2013, 96, 2042-2045.</scp>	/sçp> <sub< td=""><td>>3<s< td=""></s<></td></sub<>	>3 <s< td=""></s<>
35	Hydrothermal synthesis and mechanism and property study of La-doped BiFeO3 crystallites. Journal of Materials Science: Materials in Electronics, 2012, 23, 1402-1408.	2.2	26
36	Sol–gel hydrothermal synthesis and enhanced biosensing properties of nanoplated	6.7	41

36 lanthanum-substituted bismuth titanate microspheres. Journal of Materials Chemistry, 2011, 21, 5352.

ZHIWU CHEN

#	Article	IF	CITATIONS
37	Comparative Study of Microstructure and Electrical Properties of Varistors Prepared from Plasma Vaporâ€Phase Reaction Process and French Process ZnO Powders. Journal of the American Ceramic Society, 2011, 94, 3871-3876.	3.8	7
38	Lowâ€ŧemperature preparation of bismuth ferrite microcrystals by a solâ€gelâ€hydrothermal method. Crystal Research and Technology, 2011, 46, 309-314.	1.3	10
39	Low-temperature preparation of lanthanum-doped BiFeO3 crystallites by a sol–gel-hydrothermal method. Ceramics International, 2011, 37, 2359-2364.	4.8	52
40	Direct electrochemistry of myoglobin immobilized on chitosan-wrapped rod-constructed ZnO microspheres and its application to hydrogen peroxide biosensing. Journal of Solid State Electrochemistry, 2010, 14, 923-930.	2.5	15
41	Low-temperature preparation of nanoplated bismuth titanate microspheres by a sol–gel-hydrothermal method. Journal of Alloys and Compounds, 2010, 497, 312-315.	5.5	19
42	Hydrothermal synthesis and characterization of Bi4Ti3O12 powders. Journal of the Ceramic Society of Japan, 2009, 117, 264-267.	1.1	8
43	SnO2-based varistors capable of withstanding surge current. Journal of the Ceramic Society of Japan, 2009, 117, 851-855.	1.1	24
44	Temperature dependence of dielectric properties for Sr0.3Ba0.7Bi3.7La0.3Ti4O15 ferroelectric ceramics. Journal of the Ceramic Society of Japan, 2009, 117, 217-220.	1.1	3
45	Piezoelectric and dielectric properties of (Na0.5K0.5)NbO3-Bi0.5(Na0.8K0.2)0.5TiO3 lead-free ceramics. Journal of the Ceramic Society of Japan, 2008, 116, 661-663.	1.1	12
46	Piezoelectric and Dielectric Properties of (Bi0.5Na0.5)TiO3-Ba(Zr0.04Ti0.96)O3 Lead-Free Piezoelectric Ceramics. Journal of the Ceramic Society of Japan, 2006, 114, 857-860.	1.3	20